OPEN ACCESS
Journal of Multidisciplinary Applied Natural Science Vol. 5 No. 2 (2025) https://doi.org/10.47352/jmans.2774-3047.250
Check for updates
Research Article

Allyl-Modified of Calix[4]resorcinarene Derivatives for HER2 Inhibition Agents: An In Silico Study

Anggit Fitria, Yehezkiel Steven Kurniawan, Agus Dwi Ananto, Jumina Jumina*, Eti Nurwening Sholikhah, and Harno Dwi Pranowo

Received : September 15, 2024	Revised : October 29, 2024	Accepted : November 16, 2024	Online : February 22, 2025

Abstract
Breast cancer is one of the deathliest cancer diseases for women, with high mortality cases. Since breast cancer cells overexpressed HER2 receptors, a computerized structure-based screening was conducted to identify potential HER2 inhibitors as an anti-breast cancer agent. This method can investigate the potency of proposed compounds as potential protein inhibitors. Researchers were interested in studying some synthetic macromolecules, i.e., allyl-modified calix[4]resorcinarenes, through in silico studies as HER2 inhibitors using molecular docking studies. Prospective protein-ligand complexes for HER2 inhibition were further investigated by molecular dynamics simulations for 200 ns on different binding pockets. The allyloxycalix[4]resorcinarene derivative (5A) was identified as the most potential HER2 inhibitor through a computational approach, including molecular docking studies and molecular dynamics simulations. The HER2-5A complex was relatively stable during the 200 ns molecular dynamics run. In addition, the hydrogen bonds formed between blind docking and molecular dynamics simulations are almost unchanged for the HER2-5A complex. The HER2-5A formed with two crucial amino acid residues, i.e., Asp845 and Asn850. Moreover, the data of the molecular dynamics simulations of compounds 5A and 2A demonstrate the stability of both complexes in different binding sites of HER2. These computational results are preliminary data for further synthesis and *in vitro* evaluation.

Keywords: allyl, blind docking, breast anticancer, calix[4]resorcinarene, calix[4]pyrogalloarene

1. INTRODUCTION

Cancer caused nearly 10 million deaths in 2020, which is equivalent to one in six global deaths. The most common cancers were female breast cancer, lung cancer, and prostate cancer [1]-[3]. In 2020, there were over 2.3 million new breast cancer cases with 685,000 deaths. Unfortunately, due to population growth and aging, by 2040, the annual burden of breast cancer is expected to rise to more than 3 million new cases and 1 million deaths [4]. One method of cancer treatment can be carried out with chemotherapy using therapeutic drugs. The approved therapeutic drugs for breast cancer are tamoxifen, trastuzumab, paclitaxel, capecitabine, cyclophosphamide, gemcitabine, and docetaxel, which have various side effects due to multidrug resistance cases in cancer patients. Other drug alternatives for breast cancer treatment are investigated using natural compounds and their derivatives. Even though some natural compounds and macromolecules exhibit decisive anticancer actions, their isolation process is not easy and time-consuming, with a shallow isolation percentage [5]-[7].

Presently, computer-aided drug design is a helpful tool in modern drug development. The *in silico* approach has transformed the process by offering more efficient alternatives to the traditional *in vitro* and *in vivo* methods, which are often time-consuming and expensive [8]. This study predicts how a protein (receptor) interacts with small molecules (ligands) at the binding site of target proteins, helping to assess the biological activity of a potential drug candidate [9]. The binding energy can be obtained from the docking molecular between receptor and target compounds and is used as one of the parameters to determine a potential drug candidate [10].

Among the protein receptors, human epidermal growth factor receptor 2 (HER2), ERBB2, and HER-2/neu are tyrosine kinase members of the epidermal growth factor receptor family found in the cancer cells. The HER2 comprises three components: the extracellular, transmembrane, and intracellular domains [11]. Besides, HER2 receptor is expressed in many tissues, primarily promoting

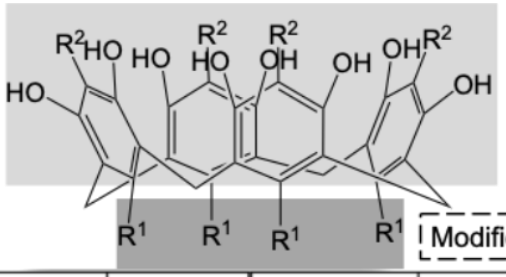

Compound	R^1	R^2	Compound	R^1	R^2
1A	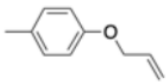	H	**4A**	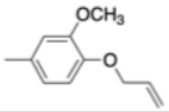	H
2A	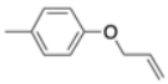	OH	**5A**	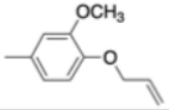	OH
3A	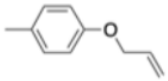	CH_3	**6A**	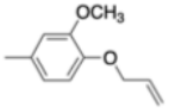	CH_3

Figure 1. Structures of proposed calix[4]resorcinarene-based ligands.

uncontrolled cell growth and tumorigenesis. The HER2 is overexpressed in about 20% of breast and gastric cancer, 16% of epithelial ovarian cancer, 20% of gastric cancer, and 1.3% of colorectal cancer [11][12]. From the biochemical perspective, HER2 contains 1255 amino acid residues with a total structural mass of 185 kDa [12]. The HER2 was deposited by Aertgeerts *et al*. with a ID of 3PP0 in the protein data bank (PDB) [13]. The HER2 gene caused crucial amplification and overexpression in the breast cancer cells. That is a critical stage that leads to the transformation of breast epithelial cells in about one-third of breast cancer patients [14].

The crystal structure of HER2 from an RCSB protein data bank can be used for computer-aided drug design to identify potential anticancer candidates [15]. For further investigation, compounds from these anticancer candidates are built and docked with the HER2 receptor to predict the binding mode and affinity between ligands and receptors used for structure-based drug design [16]. Nevertheless, molecular docking studies show a static interaction between anticancer candidates and protein receptors. On the other hand, molecular dynamics (MD) simulations provide a more detailed analysis by evaluating the stability of the complex between the targeted compound and the receptor under conditions that closely mimic the physiological environment of cells [17].

Supramolecular chemistry is noteworthy compared to natural macromolecules as anticancer agents because synthetic macromolecules can be obtained quickly and with good yield. For example, calix[4]arena with the presence of platinum(II) and L-proline is capable of various anticancers [18][19]. Conversely, calix[4]arene with the functional group of polyhydroxyamine, carbonyl amide, and trifluoromethyl aniline have been challenged as breast anticancer [20]-[22]. Recently, calix[4]arene modified with isatin and triazole groups (with an alkene group) has shown potential as an anticancer agent against MCF-7 and MDA-MB-231, with half-maximal inhibitory concentrations (IC_{50}) of 8.83 and 3.32 µM, respectively [23]. To the best of the researchers' knowledge, calix[4]arene based on resorcinol/pyrogallol exhibits remarkable biological activities such as antioxidant, antimalarial, and antibacterial [24]-[27]. These phenomena are mainly caused by more functional groups that appear on the three-dimensional structure of calix [4]arene based on resorcinol/pyrogallol compared to calix[4]arenes. However, the anticancer activity evaluation for either calix[4]resorcinarenes or calix [4]pyrogallolarenes is rarely investigated.

The reported experimental data reveal that modifying calix[4]arene with an allyl group on the lower rims enhanced the biological activity as the

Table 1. Protein-ligand interaction of the proposed ligands with the HER2 protein.

Blind docking pocket	Compd.	Binding energy (kcal mol^{-1})	Types of interaction		
			H-bond	Hydrophobic	Others
1	**1A**	-5.9030	Lys887 (2.40 Å)	Ser728, Gly729, Ala730, Phe731, Arg756, Leu807, Arg811, Lys883, Val884, Pro885, Ile886, Trp888, Gly925, Pro927, Ala928, Arg929	Pi-cation: Arg849 (4.85 Å), Carbon hydrogen bond: Lys921 (2.68 Å), Ile926 (2.81 Å)
1	**2A**	-5.9940	Val884 (5.28 Å), Ile886 (3.49 & 4.32 Å), Lys887 (4.03 Å)	Ser728, Gly729, Ala730, Phe731, Gly732, Arg756, Leu807, Asp845, Arg849, Asn850, Lys883, Pro885, Trp888, Glu914, Gly919, Ala920, Lys921, Pro922, Ala928	Carbon hydrogen bond: Lys887 (3.25 Å)
1	**3A**	-6.1080	Val884 (5.54 Å)	Ser728, Gly729, Ala730, Phe731, Arg756, Leu807, Asp808, Arg811, Asp845, Arg849, Asn850, Lys883, Pro885, Ile886, Lys887, Trp888, Glu914, Ala920, Lys921, Pro922, Ala928	Carbon hydrogen bond: Asp845 (5.21 Å)
1	**4A**	-5.9710	Arg811 (6.93 Å), Lys887 (5.91 Å)	Ser728, Ala730, Phe731, Leu807, Lys883, Val884, Pro885, Ile886, Lys887, Trp888, Lys921, Pro922, Tyr923, Asp924, Gly925, Pro927, Ala928, Arg929	Carbon hydrogen bond: Gly729 (4.79 Å), Ile926 (6.26 Å), Pi-cation: Arg849 (5.47 Å), Lys921 (5.18 Å)
1	**5A**	-5.8090	Asp845 (6.95 Å), Asn850 (4.76 Å)	Gly727, Gly729, Ala730, Gly732, Arg756, Leu807, Arg811, Val884, Pro885, Ile886, Lys887, Trp888, Lys921, Pro922, Ala928	-
1	**6A**	-5.5500	Asp845 (4.56 Å), Lys883 (5.78 Å)	Gly729, Ala730, Phe731, Gly732, Arg756, Leu807, Asp808, Arg811, Arg849, Lys883, Val884, Pro885, Ile886, Lys887, Trp888, Pro922, Lys921, Ala928	Carbon hydrogen bond: Ser728 (4.03 Å)

Table 1. *Cont.*

Blind docking pocket	Compd.	Binding energy (kcal mol^{-1})	Types of interaction		
			H-bond	Hydrophobic	Others
2	**1A**	-5.1840	-	Lys724, Val725, Gly727, Gly729, Tyr803, Gly804, Leu807, Asp808, His809, Glu812, Arg849, Leu852	Pi-cation: Arg811 (7.12 Å), Carbon hydrogen bond: Ser728 (5.12 Å), Cys805 (5.29 Å)
2	**2A**	-4.9700	Ser728 (3.28), Arg811 (4.42 Å)	Val725, Leu726, Gly727, Lys736, Leu800, Met801, Pro802, Glu804, Cys805, Leu807, Glu812, Arg849, Leu852	Pi-cation: Lys724 (6.23 Å), Asp808 (5.17 & 5.65 Å), Carbon hydrogen bond: Tyr803 (4.74 Å)
2	**3A**	-5,2150	-	Lys704, Leu726, Ser728, Pro802, Tyr803, Gly804, Cys805, Arg811, Glu812, Arg849, Leu852	Pi-anion: Asp808 (5.14 Å), Carbon hydrogen bond: Gly727 (5.72 Å), Leu807 (5.16 Å)
2	**4A**	-5.0670	Lys724 (5.94 Å), Val725 (3.74 Å), Arg811 (4.84 Å)	Gly727, Ser728, Pro802, Tyr803, Gly804, Cys805, Leu807, Glu812, Arg849, Lys921	Pi-anion: Asp808 (6.23 dan 6.24 Å), Carbon hydrogen bond: Gly727 (5.72 Å), Leu807 (5.16 Å)
2	**5A**	-4.8700	Arg811 (6.06 Å)	Val725, Leu726, Gly727, Ser728, Gly729, Ala730, Thr733, Val734, Gly804, Leu807, Asn850, Leu852, Thr862, Lys921	Pi-anion: Asp808 (6.53 dan 7.27 Å), Carbon hydrogen bond: Leu726 (6.43 Å), Arg849 (6.51 Å)
2	**6A**	-5.1780	Lys724 (5.74 Å), Cys805 (3.55 Å), Arg811 (4.04 Å),	Val725, Leu726, Gly727, Val734, Tyr803, Leu807, His809, Glu812, Arg849, Asn850, Leu852, Thr862, Lys921	Carbon hydrogen bond: Ser728 (4.76 Å), Gly804 (4.15 Å)

anticancer agent. This fact has interested us to evaluate the allyl-modified calix[4]resorcinarenes and calix[4]pyrogallolarenes as breast anticancer candidates using a computational chemistry approach. This computational approach is necessary as the preliminary screening before the actual experimental examinations to suppress the experimental cost and trials and errors. Molecular docking is a simulation of molecular interactions that predicts the binding mode and affinity between receptors and ligands used for structure-based drug design [16]. In the present work, a modification of calix[4]resorcinarenes derived from Indonesian natural products, i.e., 4-hydroxybenzaldehyde and 4 -hydroxy-3-methoxybenzaldehyde (vanillin), was carried out on the lower rim with a conversion of the hydroxyl group to an allyl group in the confidence of increasing the biological activity compared to original compounds. The proposed compound to be carried out is presented in Figure 1. This study investigated the supramolecular allyl-modified calix[4]resorcinarene derivatives docked by blind docking to the HER2 receptor. Protein-ligand interactions with low binding energy in the presence of hydrogen bonds with critical amino acid residues in the HER2 binding site were further investigated using MD simulations.

2. MATERIALS AND METHODS

2.1. Materials

The crystal structure of the kinase domain of HER2 bound with a ligand 2-{2-[4-({5-chloro-6-[3-(trifluoromethyl)phenoxy]pyridin-3-yl}amino)-5*H*-pyrrolo[3,2d]pyri-midin-5-yl]ethoxy}ethanol (PDB ID: 3PP0) having a resolution of 2.25 Å was

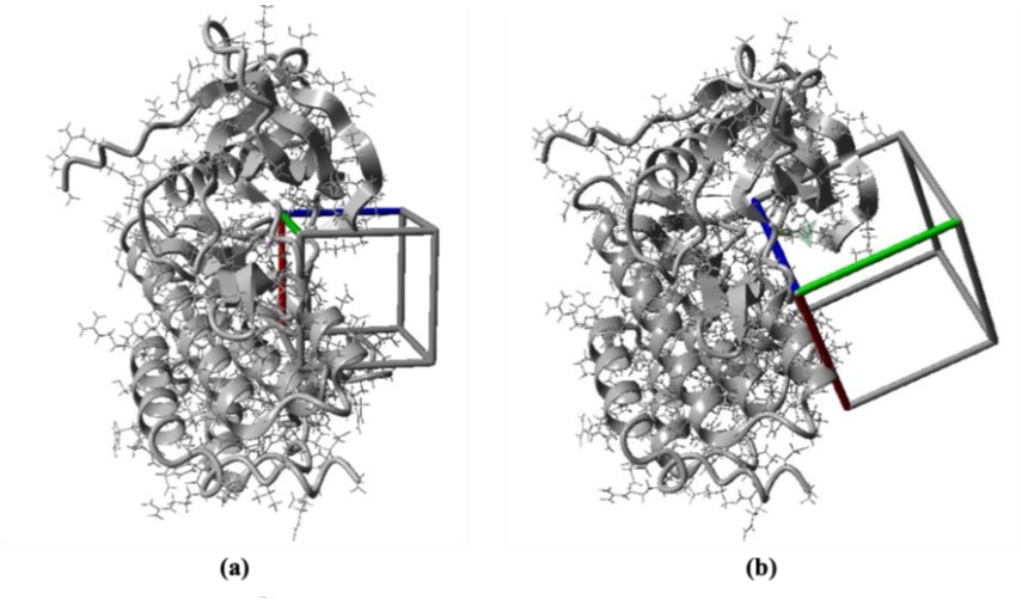

Figure 2. Blind docking (a) pocket 1 and (b) pocket 2 of HER2 receptor.

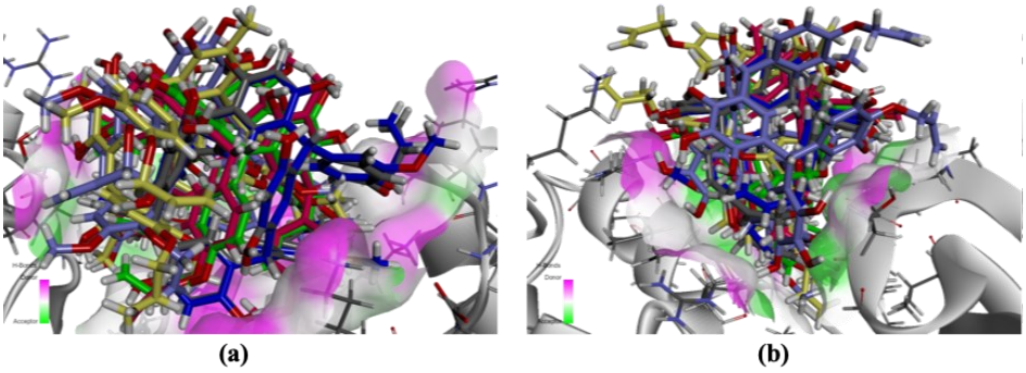

Figure 3. Stacking positions of all proposed ligands in blind docking (a) pocket 1 and (b) pocket 2 on HER2 receptor.

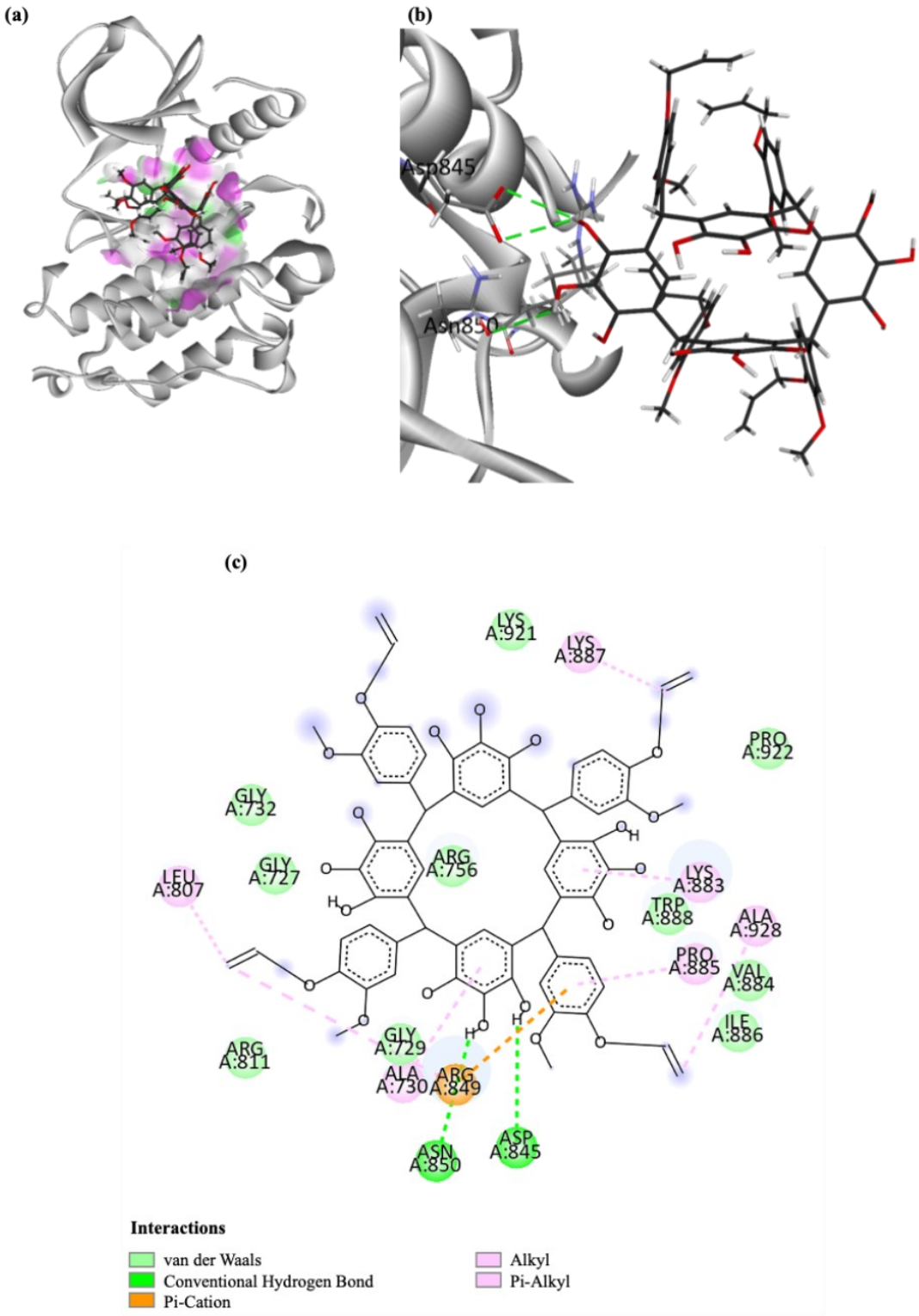

Figure 4. (a) Whole 3D structure, (b) 3D-, and (c) 2D-intermolecular interactions between compound **5A** and the HER2.

obtained from RCSB PDB website https://www.rcsb.org. Four allyloxycalix[4]resorcinarene derivatives (**1A**, **2A**, **4A**, and **5A**) and two allyloxycalix[4]pyrogallolarene derivatives (**3A** dan **6A**) are selected as the studied ligands in this work whereas their chemical structures are shown in Figure 1.

2.2. Methods

2.2.1. Optimization and Preparation of Ligands

The three-dimensional structure of allyloxyalix [4]resorcinarene and allyloxycalix[4] pyrogallolarene derivatives (**1A**–**6A**) were drawn using GaussView 5.0 software. Their structures were optimized using the density-functional theory (DFT) level with Becke's three-parameter hybrid exchange functional [28] combined with Lee, Yang, and Parr's correlation functional (B3LYP) [29], and the 6-31G basis set [30]. The final conformational structure of all compounds was obtained in boat/ flattened cone conformation as similar as possible to the experimental data following the single crystal X-ray data for stable calix[4]resorcinarene compound derivatives with this conformer [31][32]. Native ligand and compounds **1A**–**6A** were set up by adding hydrogen atoms and minimizing energy using Yet Another Scientific Artificial Reality Application (YASARA Structure) software. Each compound was saved and compiled in YOB and PDB file format.

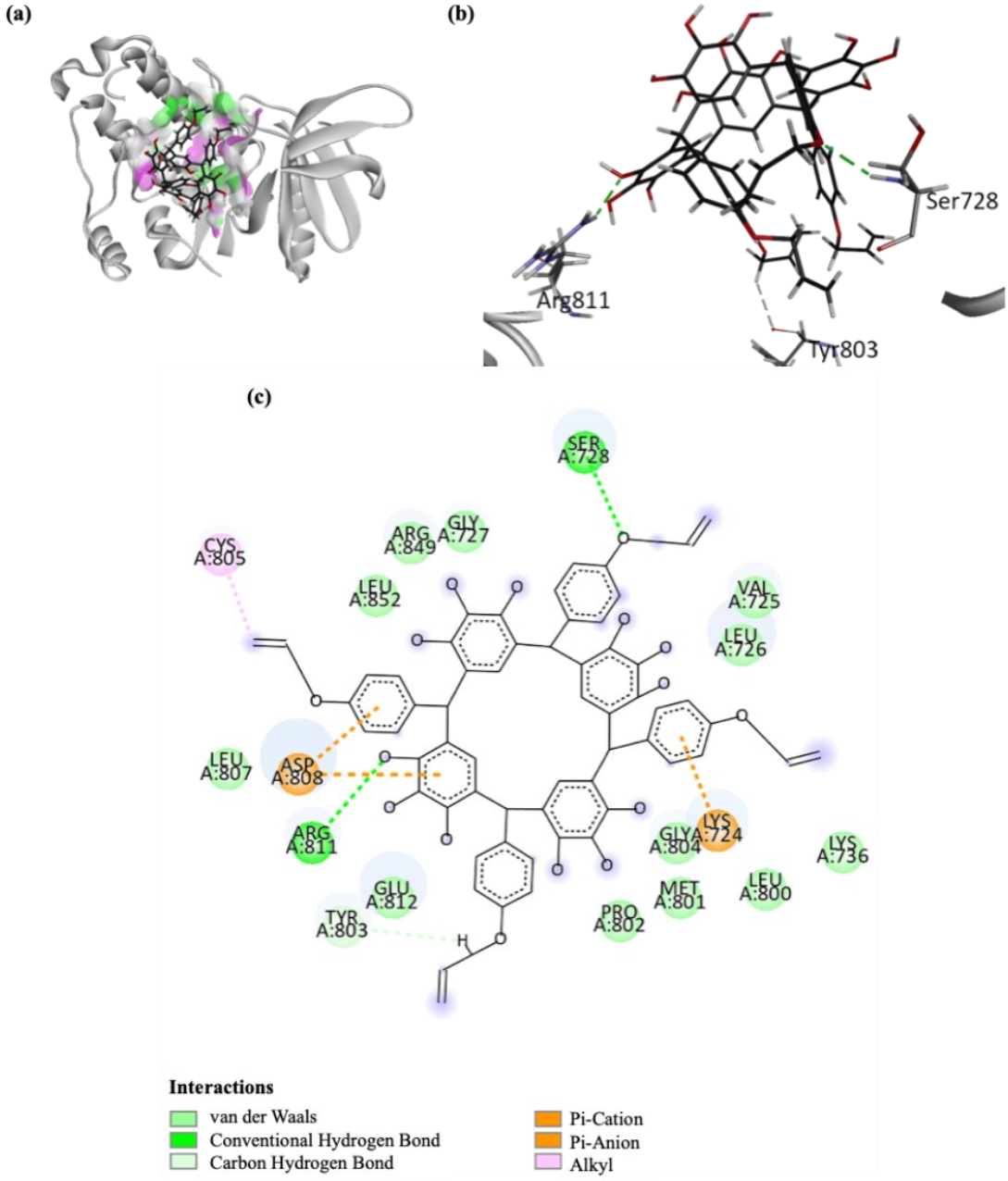

Figure 5. (a) Whole 3D structure, (b) 3D-, and (c) 2D-intermolecular interactions between compound **2A** and the HER2.

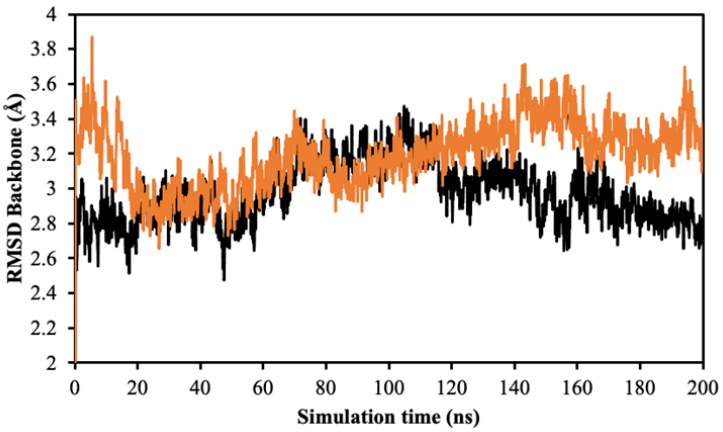

Figure 6. RMSD backbone of compound **5A** in binding pocket 1 (black) and compound **2A** in binding pocket 2 (orange) of HER2 receptor.

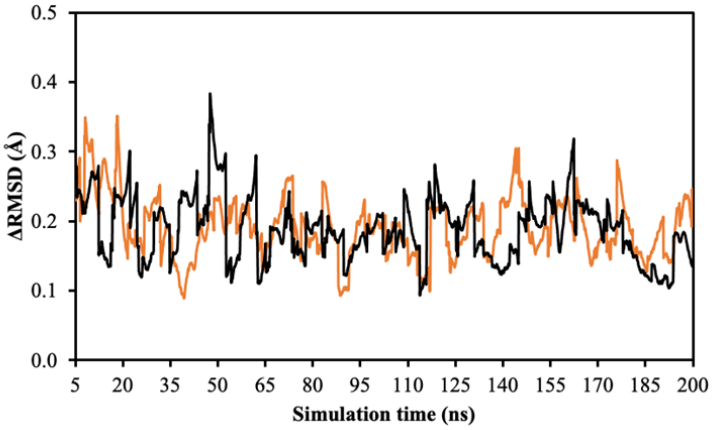

Figure 7. ΔRMSD of compound **5A** in binding pocket 1 (black) and compound **2A** in binding pocket 2 (orange) of HER2 receptor.

2.2.2. Preparation of Receptor Tyrosine-Protein

The structure file of protein and native ligand from PDBs was prepared by eliminating water molecules, side chains, and all the non-standard residues. By selecting the native ligand, the defined simulation cell could be determined through the selected cube shape with size 5 Å from the coordinates (x, y, and z) of the native ligand. Afterward, the native ligand was removed, and the receptor with SimCELL was generated. That receptor-SimCELL was saved YOB file format.

2.2.3. Docking Protein-Ligand

VINA-based YASARA Structure software was used for molecular docking study [33]. The optimized receptor and ligand files were used to set a target and play a macro. The macro file, dock_runscreening.mcr (available at http://www.yasara.org/dock_runscreeening.mcr) was used for screening and calculating energy between selected ligands with receptors to search for the druggable binding sites on the HER2 receptor. The target blind docking pocket was run for each compound using the macro file dock_run.mcr (available at http://www.yasara.org/dock_run.mcr). The docking runs of each ligand were adjusted to 100 VINA. The result log files showed that the shortening of docked complexes was completed based on binding energy (kcal mol^{-1}). The docked complexes were converted into a PDB file to visualize the complexes using BIOVIA Discovery Studio Visualizer software.

2.2.4. Molecular Dynamics Simulation

The best protein-ligand complex in PDB file format from two blind docking pockets was selected and carried out using molecular dynamics simulations. The macro file md_runmembrane.mcr

(available at http://www.yasara.org/md_runmembrane.mcr) was used for the simulation. The HER2 receptor, the ligands, and the water molecules were computed with AMBER14, GAFF2, and AM1BCC, as well as TIP3P force fields, respectively. The simulation box was adjusted to 100 × 100 × 100 Å. Similar physiological conditions also were applied for the simulation (i.e., temperature at 310 K, pressure at 1 atm (NPT ensemble), pH 7.4, and 0.9% NaCl). In this study, the duration of MD simulations run was 200 ns with a timestep of 2.5 fs and the snapshots interval of 0.1 ns. The system was first minimized using the steepest descent method and further optimized through simulated annealing to reach a density of 0.999 g mL^{-1}. An initial equilibration phase lasting 250 ps was conducted to stabilize the system. The van der Waals forces were limited to a cut-off of 8 Å, while electrostatic interactions were calculated using the Particle Mesh Ewald method without a cut-off. The complex results of the dynamics simulations were analyzed by running md_analyzer.mcr (available at http://www.yasara.org/md_analyzer.mcr) and converted respectively to PDB file format. Analysis of the snapshots included evaluations of docked and molecular mechanics/Poisson-Boltzmann surface area (MM/PBSA) binding energy, RMSD, radius of gyration (RoG), root-mean-square fluctuation (RMSF), and solvent-accessible surface area (SASA).

3. RESULTS AND DISCUSSIONS

3.1. Molecular Docking Studies

The advantages of the molecular docking approach are helpful in two conditions, i.e., before and after experimental screening [34].

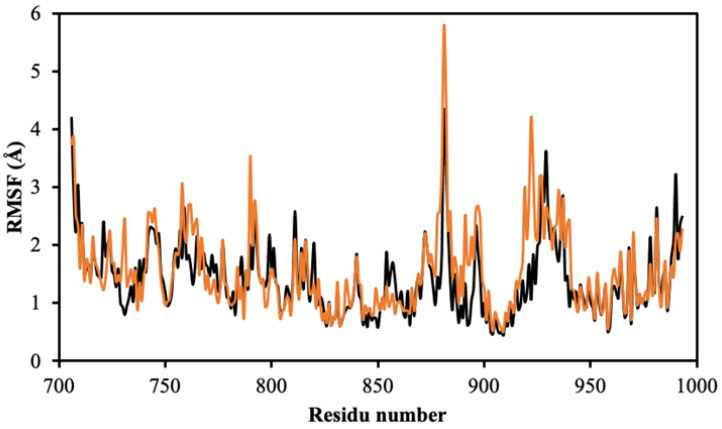

Figure 8. RMSF of compound **5A** in binding pocket 1 (black) and compound **2A** in binding pocket 2 (orange) of HER2 receptor.

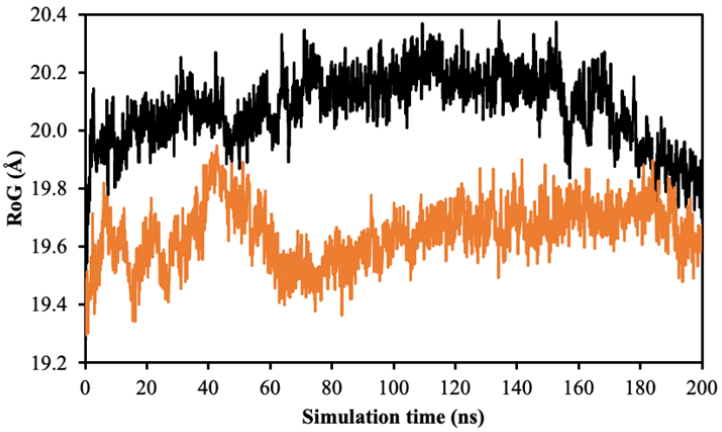

Figure 9. RoG of compound **5A** in binding pocket 1 (black) and compound **2A** in binding pocket 2 (orange) of HER2 receptor.

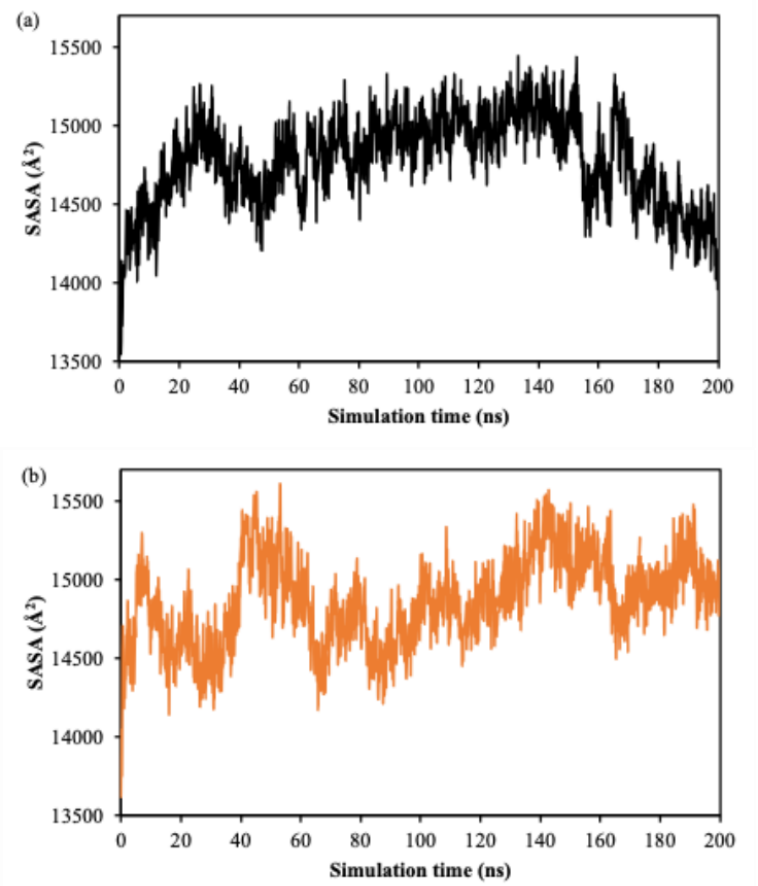

Figure 10. (a) SASA of compound **5A** in binding pocket 1 (black) and (b) compound **2A** in binding pocket 2 (orange) of HER2 receptor.

Table 2. MM/PBSA calculation for compounds **5A** and **2A** after MD simulations against HER2.

Energy	Energy value (kJ mol^{-1})	
	Compound 5A	**Compound 2A**
Energy potential receptor +	-11088.90 ± 683.42	-11464.84 ± 721.05
Energy solvation receptor +	-26457.23 ± 927.28	-26243.45 ± 1011.49
Energy potential ligand +	782.53 ± 54.99	336.81 ± 43.60
Energy solvation ligand -	-672.89 ± 50.38	-636.92 ± 41.46
Energy potential complex -	-10715.83 ± 709.08	-11347.23 ± 745.97
Energy solvation complex	-26468.73 ± 944.39	-26468.32 ± 1041.24
Binding energy	-251.92 ± 78.36	-192.85 ± 58.53

Consequently, molecular docking is beneficial in compound screening, provides a better understanding of the mechanism of action against targeted receptors, and reduces costs for developing new drugs [35]. The allyloxycalix[4]resorcinarene and allyloxycalix[4]pyrogallolarene derivatives are evaluated as ligands to target the HER2 receptor, which is overexpressed in breast cancer. Therefore, the binding mode of the proposed compound on the HER2 receptor can be used as a guide for *in silico* screening.

Allyloxycalix[4]resorcinarene and allyloxycalix [4]pyrogalloarene derivatives are supramolecules with a molecular weight of more than 1000 g mol^{-1}, which is two-fold from the native ligand, so they cannot replace the exact position of the native ligand. Therefore, we employed a blind docking approach, which is proper for determining the

interactions of the compound with the target protein [36]. The docking results of allyloxycalix[4] resorcinarene and allyloxycalix[4]pyrogallolarene derivatives were ordered based on the binding energy shown in Table 1. This research was carried out through a blind docking approach, whereas the proposed compound docked in a position different from that of the native ligand. Two blind docking pockets allow the proposed compounds to dock properly at the HER2 receptor (Figure 2). The blind docking results of the proposed compound in pocket 1 (Figure 3(a)) show that the formed conformers formed are random. In contrast to pocket 2 (Figure 3(b)), the conformers of each compound give almost the same pocket direction.

Table 1 shows that compounds **1A**–**6A** generated a binding energy of 5.5500–6.1080 kcal mol^{-1} on the blind docking pocket 1 while they generated a lower binding energy of 4.8700–5.2150 kcal mol^{-1} on the blind docking pocket 2. The Asp845 amino acid plays a crucial role as an active site of the HER2 receptor. The Asp845 acts as a catalytic loop for the HER2, associated with other amino acids (Arg844–Asn850) [13]. However, only compound **5A** generated an active site with Asp845 through hydrogen bonds and another hydrogen bond with Asn850 with a binding energy of 5.8090 kcal mol^{-1}. Figure 3(a) shows a promising conformer of **5A** to HER2 by blind docking pocket 1. The lower rim of **5A** was modified by the presence of allyl groups providing hydrophobic interactions with Gly727, Gly729, Ala730, Gly732, Arg756, Leu807, Arg811, Val884, Pro885, Ile886, Lys887, Trp888, Lys921, Pro922, and Ala928 residues (Figure 4(b)). Thus, the allyl group is expected to provide additional inhibitory activity to the HER2 protein.

Compound **2A** interacts with the binding site on the blind docking pocket 2, i.e., Leu800 and Leu852 via hydrophobic interaction. The binding energy of **2A** is 4.9700 kcal mol^{-1} with two conventional hydrogen bonds formed with Ser728 and Arg811 residues with a distance of 3.28 and 4.42 Å, respectively (Figure 5(b)). The Ser728 is the glycine-rich nucleotide phosphate-binding loop associated with the catalytic activity [13]. Compound **2A** showed the hydrophobic interactions towards the amino acid residues of Val725, Leu726, Gly727, Lys736, Leu800, Met801, Pro802, Glu804, Cys805, Leu807, Glu812, Arg849, and Leu852, as well as showed pi-cation with Lys724 and Asp808, and carbon hydrogen bond with Tyr803. Therefore, the molecular docking results propose two potential HER2 inhibitor candidates, i.e., compound **5A** in the binding pocket 1 and compound **2A** in the binding pocket 2 of the HER2 receptor.

3.2. MD Simulations

Molecular docking describes the ligand in a flexible state while the protein is in a fixed state so that one position of the ligand-protein complex is obtained. Meanwhile, MD allows flexible conformational changes in ligand and protein structures at artificial physiological conditions. The ligand and amino acid residues can interact for a particular simulation period [37]. The MD simulations follow the selected blind docking results to investigate the dynamic stability of the compound in the dynamic system compared with the docking results. After a 200 ns simulation, the RMSD values of compound **5A** in the binding

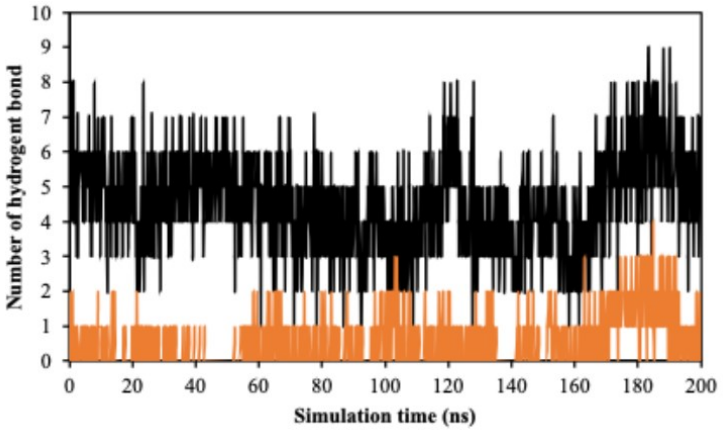

Figure 11. Number of hydrogen bonds in complex (a) HER2-**5A** (black) and (b) HER2-**2A** (orange).

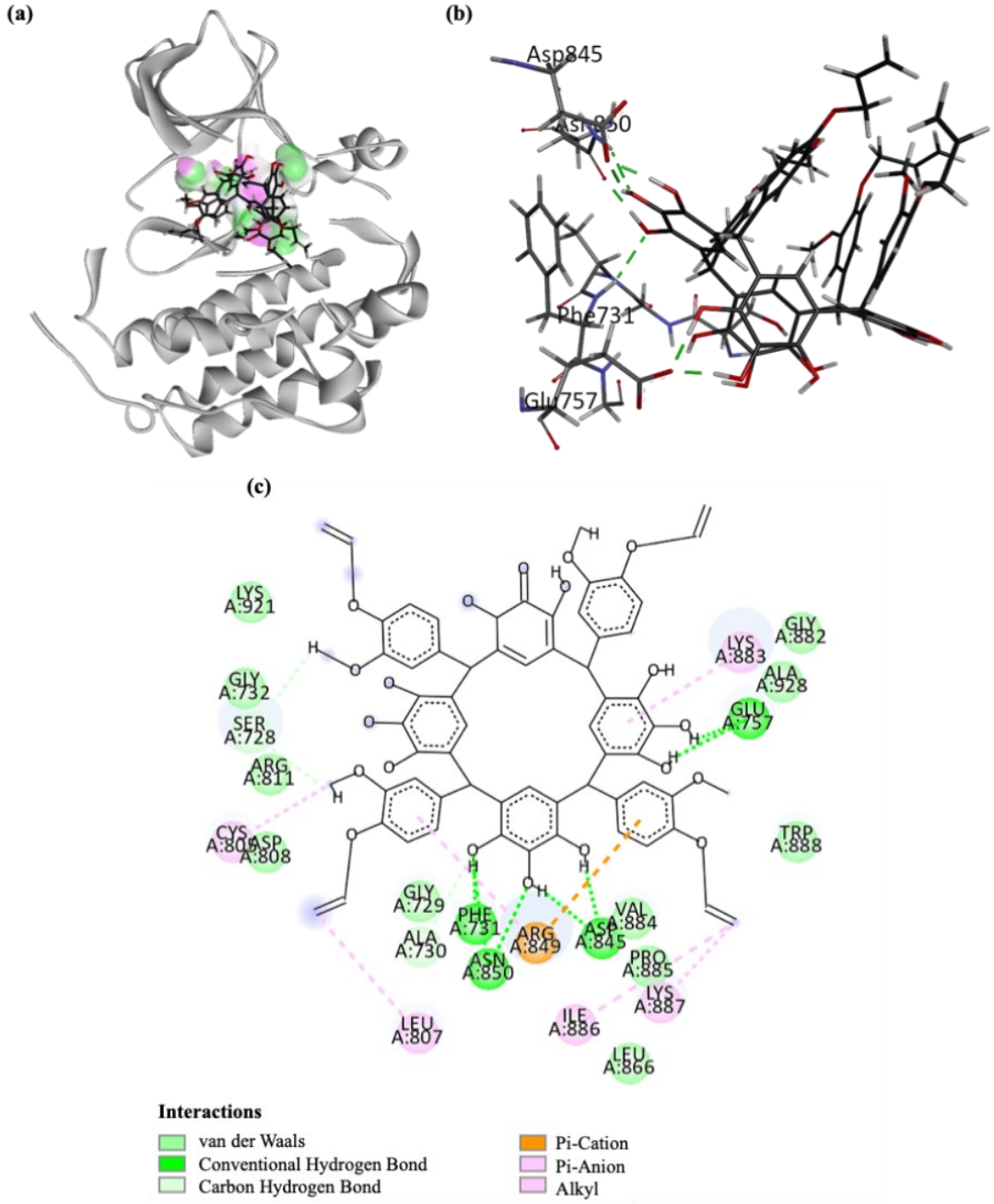

Figure 12. (a) Whole 3D structure, (b) 3D-, and (c) 2D-intermolecular interactions between **5A** and the HER2 at 200 ns.

pocket 1 and compound **2A** in the binding pocket 2 of the HER2 receptor are shown in Figure 6. The RMSD value of compound **5A** was lower than compound **2A**. The RMSD value **5A** during the MD simulation run ranged from 0.63 to 3.47 Å, with the average RMSD value of 2.97 Å. Also, **2A** during the MD simulation run, the backbone RMSD value had a range of 0.59 to 3.86 Å with an average value of 3.19 Å. However, both ΔRMSD values at every five ns were satisfied, i.e., less than 0.4 Å (Figure 7), demonstrating that the backbone structures of the compounds and HER2 receptor were stable during the MD simulations.

In describing fluctuations of amino acid residues, RMSF analysis shows changes in proteins and amino acids that contribute to interactions between ligand-protein complexes. A significant RMSF value indicates the protein-ligand complex is unstable and flexible, while a small RMSF value indicates a more stable complex [38]. Based on the data in Figure 8, the average RMSF value of the HER2-**5A** complex is 1.42 Å. The HER2-**5A**

complex fluctuated up to 4.30 Å at amino acid residue 881. The RMSF value of HER2-**5A** reached its lowest point at 0.45 with residue 909. Fortunately, RMSF values of the binding pocket of **5A** remained stable, i.e., 1.53 Å at residue 800, 0.59 Å at residue 845, and 1.04 Å at residue 852. Meanwhile, the average RMSF value of the HER2-**2A** complex was 1.55 Å. The RMSF pattern showed a fluctuating graph, reaching the highest value of 5.77 Å at residue 881. The HER2-**2A** complex indicated the lowest RMSF value of 0.50 Å at residue 909. Fortunately, RMSF values of the binding pocket of **2A** remained stable, i.e., 1.59 Å at residue 800, 0.85 Å at residue 845, and 1.09 Å at residue 852. The RMSF values of **5A** and **2A** showed that the interaction of both compounds in the active site of the HER2 receptor remained stable.

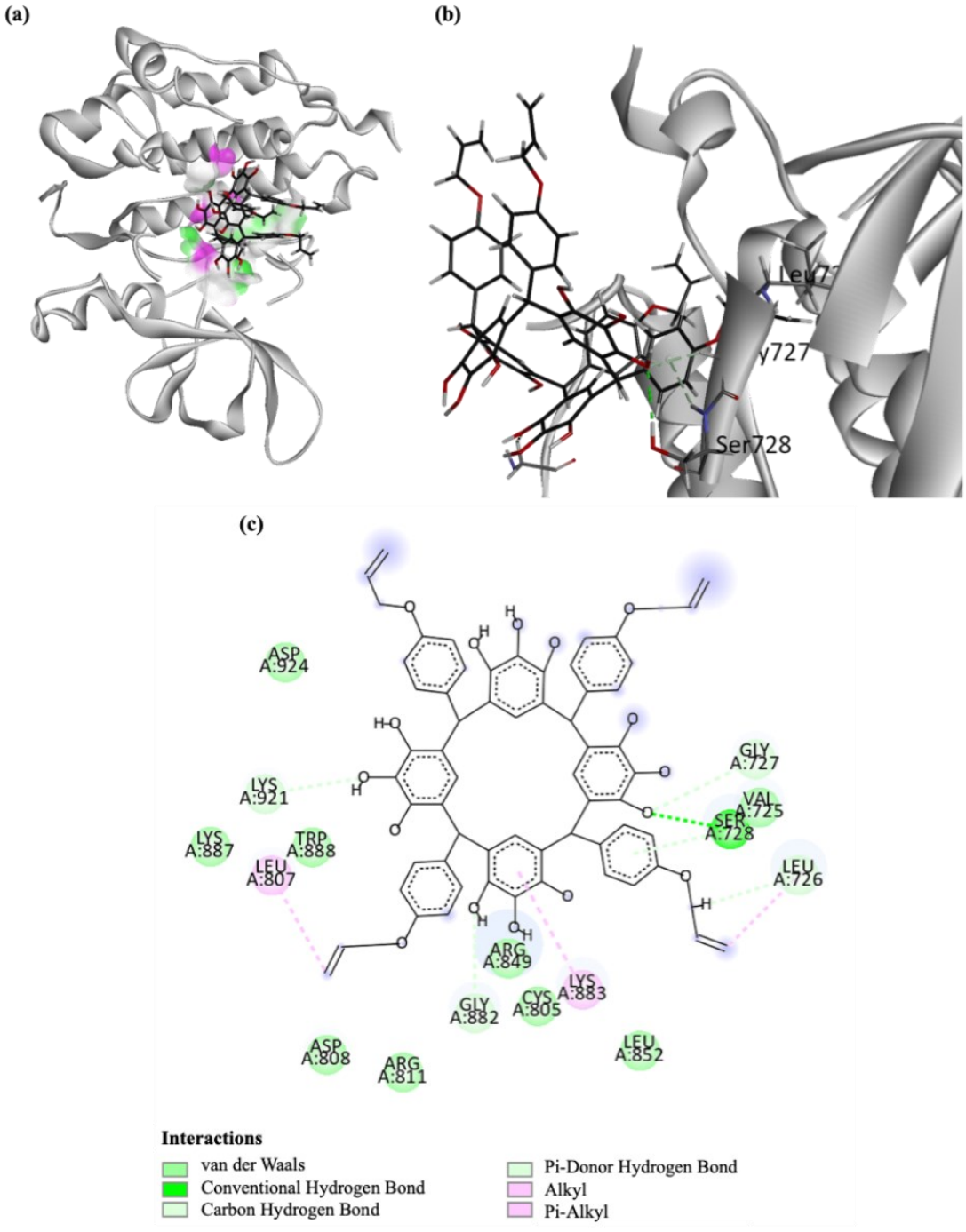

Figure 13. (a) Whole 3D structure, (b) 3D-, and (c) 2D-intermolecular interactions between **2A** and the HER2 at 200 ns.

The RoG is also needed to check the stability of the protein structure by looking at the level of protein compactness. A significant amplitude value indicates a loosely arranged protein and a small amplitude value indicates a compactly arranged protein [39]. The RoG values are shown in Figure 9. The RoG values of the HER2-**5A** complex ranged from 19.21 to 20.37 Å. Meanwhile, the HER2-**2A** complex has RoG values ranging from 19.29 to 19.97 Å. The RoG value of both compounds was not significantly different and was relatively stable during the MD simulations.

On the other hand, the SASA value represents the accessible surface area of the protein complex for each ligand, as shown in Figure 10. The SASA data of compound **5A** ranged from 13,512.92 to 15,448.74 $Å^2$. The SASA data of compound **2A** ranged from 13,615.12 to 15,611.57 $Å^2$, which was in line with the RoG value and was stable during the simulations.

The binding energy from MD simulations for protein-ligand interaction is calculated using MM/PBSA and the results are shown in Table 2. The binding energy is the combination of molecular mechanics energy and solvation energy (Poisson–Boltzmann [PB] and surface area [SA]) of receptor, ligand, and complex of receptor-ligand [40]. The binding energy value of the HER2-**5A** complex (-251.92 ± 78.36 kJ mol^{-1}) is lower than the HER2-**2A** complex (-192.85 ± 58.53 kJ mol^{-1}). This indicates the HER2-**5A** complex is more stable during the MD simulation.

The chemical interactions of compound **5A** after MD simulations are illustrated in Figures 11 and 12. After a 200 ns simulation, compound **5A** established hydrogen bonds with Asp845 and Asn850 as the catalytic loop and additional hydrogen bonds with Phe731 (2.34 Å) and Glu757 (1.62 and 1.73 Å). More observed hydrogen bonds between the protein and the ligand indicate a stronger binding affinity [39]. The hydrogen bond distances with Asp845 and Asn850 residues were 1.70–1.72 and 2.08 Å (from MD simulation results) compared to 6.95 and 4.76 Å (from molecular docking results). The data showed that the hydrogen bonds to residues Asp845 and Asn850 become more potent, as revealed by the shorter hydrogen bond distances during 200 ns simulations. Other interactions are observed including carbon-hydrogen bonds with Ser728 and Ala730, hydrophobic interactions involving Cys805, Leu807, and Arg849, and a pi-cation interaction with Arg849. These new interactions resulted in lower binding energy, as determined by the MM/PBSA method (Table 2), than the molecular docking binding energy (-5.81 kcal mol^{-1}).

Similarly, the chemical interactions of compound **2A** following MD simulations are shown in Figure 13. After a 200 ns simulation, compound **2A** formed a hydrogen bond with Ser728, along with carbon-hydrogen bonds with Gly721, Val725, Leu726, Gly882, and Lys921, as well as hydrophobic interactions with Leu726, Leu807, and Lys883. The hydrogen bond distance with Ser728 was found to be 4.40 Å (from MD simulation results) compared to 3.28 Å (from molecular docking results). Also, Arg811 residue disappeared in the end of the simulation. This proves that the hydrogen bond during docking is unstable, as indicated by a change in interaction with the amino acid residue. These interactions also led to lower binding energy, calculated by the MM/PBSA method (Table 2), compared to the molecular docking binding energy (-4.97 kcal mol^{-1}). Figure 11 depicts the number of hydrogen bonds formed by compounds **5A** and **2A** throughout the 200 ns simulation. It can be concluded that **5A** binds more substantially to the HER2 receptor compared to **2A** and is expected to have a higher anticancer activity. However, further confirmation of the mechanism of action of **5A** against HER2 shall be investigated in the future.

4. CONCLUSIONS

Allyloxycalix[4]resorcinarene and allyloxycalix[4]pyrogalloarene derivatives were blindly docked in the active site of HER2 protein. The final MD simulations show that compound **5A** generated 4 hydrogen bonds with HER2 receptor through Phe731, Glu757, Asn845, and Asn850. Nevertheless, the HER2-**2A** complex only made a hydrogen bond with Ser728. From the results of 200 ns simulations, compound **5A** gave stronger binding energy (-251.92 ± 78.36 kJ mol^{-1}) than compound **2A** (-192.85 ± 58.53 kJ mol^{-1}) due to more available functional group of compound **5A**

on the active site of HER2 receptor. The lower binding energy of compound **5A** was generated from more hydrogen bonds formed during the MD simulations. In molecular docking and MD simulations, only compound **5A** interacted with the crucial amino acid residues, i.e., Asn845 and Asn850. Moreover, the RMSD, RMSF, RoG, and SASA of compounds **5A** and **2A** demonstrate the stability of both complexes in different binding sites of HER2.

AUTHOR INFORMATION

Corresponding Author

Jumina Jumina — Department of Chemistry, Universitas Gadjah Mada, Yogyakarta-55281 (Indonesia);
orcid.org/0000-0003-2604-7838
Email: jumina@ugm.ac.id

Authors

Anggit Fitria — Department of Chemistry, Universitas Gadjah Mada, Yogyakarta-55281 (Indonesia);
orcid.org/0000-0001-7535-8160

Yehezkiel Steven Kurniawan — Department of Chemistry, Universitas Gadjah Mada, Yogyakarta-55281 (Indonesia);
orcid.org/0000-0002-4547-239X

Agus Dwi Ananto — Department of Chemistry, Universitas Gadjah Mada, Yogyakarta-55281 (Indonesia);
orcid.org/0009-0003-9276-4242

Eti Nurwening Sholikhah — Department of Pharmacology and Therapy, Universitas Gadjah Mada, Yogyakarta-55281 (Indonesia);
orcid.org/0000-0002-6545-8691

Harno Dwi Pranowo — Department of Chemistry, Universitas Gadjah Mada, Yogyakarta-55281 (Indonesia);
orcid.org/0000-0002-0223-5036

Author Contributions

Conceptualization, J. J. and H. D. P.; Methodology, H. D. P.; Software, H. D. P. and A. D. A.; Validation, J. J. and H. D. P.; Formal Analysis, A. F., Y. S. K., and A. D. A.; Investigation, A. F., Y. S. K., and A. D. A.; Resources, H. D. P.; Data Curation, A. F., Y. S. K., and A. D. A.; Writing – Original Draft Preparation, A. F. and Y. S. K.; Writing – Review & Editing, J. J., H. D. P., E. N. S., A. F., Y. S. K., and A. D. A.; Supervision, J. J., H. D. P. and E. N. S.; Project Administration, J. J.; Funding Acquisition, J. J.

Conflicts of Interest

The authors declare no conflict of interest.

ACKNOWLEDGEMENT

We thank the Directorate General of Higher Education, Research, and Technology, The Ministry of Education, Culture, Research, and Technology, the Republic of Indonesia for funding this research through Penelitian Disertasi Doktor (PDD) Grant 2023 No. 122/E5/PG.02.00.PL/2023. Special thanks are extended to the Austrian-Indonesian Centre (AIC) for Computational Chemistry for providing GaussView 5.0 licenses and to Agus Dwi Ananto for providing YASARA Structure licenses.

REFERENCES

[1] J. Ferlay, M. Colombet, I. Soerjomataram, D. M. Parkin, M. Pineros, A. Znaor, and F. Bray. (2021). "Cancer statistics for the year 2020: An overview". *International Journal of Cancer.* 10.1002/ijc.33588.

[2] R. L. Siegel, K. D. Miller, H. E. Fuchs, and A. Jemal. (2022). "Cancer statistics, 2022". *CA: a Cancer Journal for Clinicians.* **72** (1): 7-33. 10.3322/caac.21708.

[3] Y. S. Kurniawan, K. Gurning, I. Iksen, and A. Bikharudin. (2024). "Fight for Cancer Diseases using Natural Compounds and Their Semisynthetic Derivatives". *Bioactivities.* 10.47352/bioactivities.2963-654X.221.

[4] M. Arnold, E. Morgan, H. Rumgay, A. Mafra, D. Singh, M. Laversanne, J. Vignat, J. R. Gralow, F. Cardoso, S. Siesling, and I. Soerjomataram. (2022). "Current and future burden of breast cancer: Global statistics for 2020 and 2040". *Breast.* **66** : 15-23. 10.1016/j.breast.2022.08.010.

[5] T. Fujii, R. Yajima, H. Tatsuki, K. Oosone, and H. Kuwano. (2016). "Anticancer effect of rapamycin on MCF-7 via downregulation of VEGF expression". *In Vitro Cellular &*

Developmental Biology. **52** (1): 45-8. 10.1007/s11626-015-9944-5.

[6] R. Acharya, S. Chacko, P. Bose, A. Lapenna, and S. P. Pattanayak. (2019). "Structure Based Multitargeted Molecular Docking Analysis of Selected Furanocoumarins against Breast Cancer". *Scientific Reports.* **9** (1). 10.1038/s41598-019-52162-0.

[7] S. A. Elseginy, R. Hamdy, V. Menon, A. M. Almehdi, R. El-Awady, and S. S. M. Soliman. (2020). "Design, synthesis, and computational validation of novel compounds selectively targeting HER2-expressing breast cancer". *Bioorganic & Medicinal Chemistry Letters.* **30** (24): 127658. 10.1016/j.bmcl.2020.127658.

[8] M. R. Hasan, A. A. Alsaiari, B. Z. Fakhurji, M. H. R. Molla, A. H. Asseri, M. A. A. Sumon, M. N. Park, F. Ahammad, and B. Kim. (2022). "Application of Mathematical Modeling and Computational Tools in the Modern Drug Design and Development Process". *Molecules.* **27** (13). 10.3390/molecules27134169.

[9] M. Z. Nawaz, S. A. Attique, Q. U. Ain, H. A. Alghamdi, M. Bilal, W. Yan, and D. Zhu. (2022). "Discovery and characterization of dual inhibitors of human Vanin-1 and Vanin-2 enzymes through molecular docking and dynamic simulation-based approach". *International Journal of Biological Macromolecules.* **213** : 1088-1097. 10.1016/j.ijbiomac.2022.06.014.

[10] Y. S. Kurniawan, N. Fatmasari, J. Jumina, H. D. Pranowo, and E. N. Sholikhah. (2023). "Evaluation of The Anticancer Activity of Hydroxyxanthones Against Human Liver Carcinoma Cell Line". *Journal of Multidisciplinary Applied Natural Science.* **4** (1): 1-15. 10.47352/jmans.2774-3047.165.

[11] X. Xia, C. Gong, Y. Zhang, and H. Xiong. (2023). "The History and Development of HER2 Inhibitors". *Pharmaceuticals (Basel).* **16** (10). 10.3390/ph16101450.

[12] N. Iqbal and N. Iqbal. (2014). "Human Epidermal Growth Factor Receptor 2 (HER2) in Cancers: Overexpression and Therapeutic Implications". *Molecular Biology International.* **2014** 852748. 10.1155/2014/852748.

[13] K. Aertgeerts, R. Skene, J. Yano, B. C. Sang, H. Zou, G. Snell, A. Jennings, K. Iwamoto, N. Habuka, A. Hirokawa, T. Ishikawa, T. Tanaka, H. Miki, Y. Ohta, and S. Sogabe. (2011). "Structural analysis of the mechanism of inhibition and allosteric activation of the kinase domain of HER2 protein". *Journal of Biological Chemistry.* **286** (21): 18756-65. 10.1074/jbc.M110.206193.

[14] S. Meng, D. Tripathy, S. Shete, R. Ashfaq, B. Haley, S. Perkins, P. Beitsch, A. Khan, D. Euhus, C. Osborne, E. Frenkel, S. Hoover, M. Leitch, E. Clifford, E. Vitetta, L. Morrison, D. Herlyn, L. W. Terstappen, T. Fleming, T. Fehm, T. Tucker, N. Lane, J. Wang, and J. Uhr. (2004). "HER-2 gene amplification can be acquired as breast cancer progresses". *Proceedings of the National Academy of Sciences (PNAS).* **101** (25): 9393-8. 10.1073/pnas.0402993101.

[15] S. S. Sohrab and M. A. Kamal. (2022). "Screening, Docking, and Molecular Dynamics Study of Natural Compounds as an Anti-HER2 for the Management of Breast Cancer". *Life (Basel).* **12** (11). 10.3390/life12111729.

[16] J. Fan, A. Fu, and L. Zhang. (2019). "Progress in molecular docking". *Quantitative Biology.* **7** (2): 83-89. 10.1007/s40484-019-0172-y.

[17] Y. S. Kurniawan, E. Yudha, G. Nugraha, N. Fatmasari, H. D. Pranowo, J. Jumina, and E. N. Sholikhah. (2024). "Molecular Docking and Molecular Dynamic Investigations of Xanthone-Chalcone Derivatives against Epidermal Growth Factor Receptor for Preliminary Discovery of Novel Anticancer Agent". *Indonesian Journal of Chemistry.* **24** (1). 10.22146/ijc.88449.

[18] F. Nasuhi Pur and K. A. Dilmaghani. (2014). "Calixplatin: novel potential anticancer agent based on the platinum complex with functionalized calixarene". *Journal of Coordination Chemistry.* **67** (3): 440-448. 10.1080/00958972.2014.890718.

[19] M. Oguz, A. Gul, S. Karakurt, and M. Yilmaz. (2020). "Synthesis and evaluation of

the antitumor activity of Calix[4]arene l-proline derivatives". *Bioorganic Chemistry*. **94** : 103207. 10.1016/j.bioorg.2019.103207.

[20] L. An, C. Wang, L. Han, J. Liu, T. Huang, Y. Zheng, C. Yan, and J. Sun. (2019). "Structural Design, Synthesis, and Preliminary Biological Evaluation of Novel Dihomooxacalix[4]arene-Based Anti-tumor Agents". *Frontiers in Chemistry*. **7** : 856. 10.3389/fchem.2019.00856.

[21] L. An, C. Wang, Y. G. Zheng, J. D. Liu, and T. H. Huang. (2021). "Design, synthesis and evaluation of calix[4]arene-based carbonyl amide derivatives with antitumor activities". *European Journal of Medicinal Chemistry*. **210** : 112984. 10.1016/j.ejmech.2020.112984.

[22] M. Oguz. (2022). "Synthesis and anticancer activity of new p-tertbutylcalix[4]arenes integrated with trifluoromethyl aniline groups against several cell lines". *Tetrahedron*. **116**. 10.1016/j.tet.2022.132816.

[23] A. Oguz, B. N. Saglik, M. Oguz, B. Ozturk, and M. Yilmaz. (2024). "Novel mitochondrial and DNA damaging fluorescent Calix[4]arenes bearing isatin groups as aromatase inhibitors: Design, synthesis and anticancer activity". *Bioorganic & Medicinal Chemistry*. **98** : 117586. 10.1016/j.bmc.2023.117586.

[24] B. I. G. M. Ngurah, J. Jumina, C. Anwar, S. Sunardi, and M. Mustofa. (2017). "Synthesis and In Vitro Evaluation of C-methylcalix[4]resorcinaryl octacinnamate and C-methylcalix[4]resorcinaryl octabenzoate as the Sunscreen". *Indonesian Journal of Chemistry*. **17** (1). 10.22146/ijc.23575.

[25] J. Jumina, D. Siswanta, A. K. Zulkarnain, S. Triono, P. Priatmoko, E. Yuanita, N. Fatmasari, and I. Nursalim. (2019). "Development of C-Arylcalix[4] resorcinarenes and C-Arylcalix[4] pyrogallolarenes as Antioxidant and UV-B Protector". *Indonesian Journal of Chemistry*. **19** (2). 10.22146/ijc.26868.

[26] K. Sathiyaseelan, A. Antony Muthu Prabhu, and N. Rajendiran. (2024). "Photophysical, Antioxidant, Antibacterial and NBO, LOL, ELF Analysis of Alkyl Groups Substituted Calix[4]resorcinarenes". *Journal of Fluorescence*. **34** (2): 885-903. 10.1007/s10895-023-03280-6.

[27] R. R. Putri, H. D. Pranowo, Y. S. Kurniawan, H. A. Fatimi, and J. Jumina. (2023). "Synthesis of Calix[4]resorcinarene Derivatives as Antimalarial Agents through Heme Polymerization Inhibition Assay". *Indonesian Journal of Chemistry*. **23** (4). 10.22146/ijc.81452.

[28] A. D. Becke. (1993). "Density-functional thermochemistry. III. The role of exact exchange". *The Journal of Chemical Physics*. **98** (7): 5648-5652. 10.1063/1.464913.

[29] C. Lee, W. Yang, and R. G. Parr. (1988). "Development of the Colle-Salvetti correlation-energy formula into a functional of the electron density". *Physical Review B: Condensed Matter*. **37** (2): 785-789. 10.1103/physrevb.37.785.

[30] A. Suwattanamala, A. L. Magalhães, and J. A. N. F. Gomes. (2005). "Computational study of calix[4]arene derivatives and complexation with Zn2+". *Chemical Physics*. **310** (1-3): 109-122. 10.1016/j.chemphys.2004.10.029.

[31] Vera I. Maslennikova, Olga S. Serkova, M. Gruner, S. Goutal, I. Bauer, Wolf D. Habicher, Konstantin A. Lyssenko, Mikhail Y. Antipin, and Eduard E. Nifantyev. (2004). "Synthesis and Conformation Analysis of New Perphosphorylated Calix[4]resorcinarenes". *European Journal of Organic Chemistry*. **2004** (23): 4884-4893. 10.1002/ejoc.200400363.

[32] A. Velásquez-Silva, B. Cortés, Z. J. Rivera-Monroy, A. Pérez-Redondo, and M. Maldonado. (2017). "Crystal structure and dynamic NMR studies of octaacetyl-tetra (propyl)calix[4]resorcinarene". *Journal of Molecular Structure*. **1137** : 380-386. 10.1016/j.molstruc.2017.02.059.

[33] P. Shree, P. Mishra, C. Selvaraj, S. K. Singh, R. Chaube, N. Garg, and Y. B. Tripathi. (2022). "Targeting COVID-19 (SARS-CoV-2) main protease through active phytochemicals of ayurvedic medicinal

plants - Withania somnifera (Ashwagandha), Tinospora cordifolia (Giloy) and Ocimum sanctum (Tulsi) - a molecular docking study". *Journal of Biomolecular Structure and Dynamics.* **40** (1): 190-203. 10.1080/07391102.2020.1810778.

[34] X. Y. Meng, H. X. Zhang, M. Mezei, and M. Cui. (2011). "Molecular docking: a powerful approach for structure-based drug discovery". *Current Computer-Aided Drug Design.* **7** (2): 146-57. 10.2174/157340911795677602.

[35] M. R. Yadav, P. R. Murumkar, R. Yadav, and K. Joshi. (2023). In: "Cheminformatics, QSAR and Machine Learning Applications for Novel Drug Development". 69-88. 10.1016/b978-0-443-18638-7.00006-2.

[36] G. Grasso, A. Di Gregorio, B. Mavkov, D. Piga, G. F. D. Labate, A. Danani, and M. A. Deriu. (2022). "Fragmented blind docking: a novel protein-ligand binding prediction protocol". *Journal of Biomolecular Structure and Dynamics.* **40** (24): 13472-13481. 10.1080/07391102.2021.1988709.

[37] N. Fayyazi, A. Fassihi, S. Esmaeili, S. Taheri, J. B. Ghasemi, and L. Saghaie. (2020). "Molecular dynamics simulation and 3D-pharmacophore analysis of new quinoline -based analogues with dual potential against EGFR and VEGFR-2". *International Journal of Biological Macromolecules.* **142** : 94-113. 10.1016/j.ijbiomac.2019.09.077.

[38] F. F. Wulan, T. D. Wahyuningsih, E. Astuti, and N. Prasetyo. (2024). "Towards targeting EGFR and COX-2 inhibitors: comprehensive computational studies on the role of chlorine group in novel thienyl-pyrazoline derivative". *Journal of Biomolecular Structure and Dynamics.* **42** (19): 9857-9872. 10.1080/07391102.2023.2252915.

[39] M. Surti, M. Patel, M. Adnan, A. Moin, S. A. Ashraf, A. J. Siddiqui, M. Snoussi, S. Deshpande, and M. N. Reddy. (2020). "Ilimaquinone (marine sponge metabolite) as a novel inhibitor of SARS-CoV-2 key target proteins in comparison with suggested COVID-19 drugs: designing, docking and molecular dynamics simulation study". *RSC Advances.* **10** (62): 37707-37720. 10.1039/d0ra06379g.

[40] N. Homeyer and H. Gohlke. (2012). "Free Energy Calculations by the Molecular Mechanics Poisson-Boltzmann Surface Area Method". *Molecular Informatics.* **31** (2): 114-22. 10.1002/minf.201100135.